



OPEN

Quantitative assessment of abdominal ectopic fat deposits in patients with different glucose tolerance by using mDixon Quant MRI

Bingshuo Yuan^{1,2,5}, Zhengzheng Tao^{2,5}, Yajie Ma³, Yuling Zhang³, Zhiqiang Chu⁴✉ & Qian Ji²✉

This study aimed to quantitatively analyze the characteristics of abdominal ectopic fat deposition in patients with different glucose tolerance by using mDixon Quant MRI. A total of 98 patients and 38 healthy volunteers were included in this study. The patients were stratified as impaired glucose tolerance (IGT) group ($n = 18$), the duration of diabetes less than 5 years (DMa group, $n = 31$) and longer than 5 years (DMb group, $n = 49$). The fat fraction (FF) of left hepatic lobe, right hepatic lobe, whole liver, pancreatic head, pancreatic body, pancreatic tail, spleen, kidney, as well as L3 vertebra, psoas muscle, the total abdominal fat area (S1), intra-abdominal fat area (S2) and S3 (S2/S1) were measured and calculated separately. Analysis of variance, correlation analysis, paired sample t -test, Welch's ANOVA, ROC curve and ordered multivariate logistic regression were performed for statistical analyses. The difference in BMI and weight among the four groups were statistically significant ($P < 0.001$). The metabolic parameters were statistically significant among three patients groups ($P < 0.05$). The differences in FF values of left hepatic lobe, right hepatic lobe and whole liver, spleen, pancreatic head, pancreatic body and pancreatic tail, L3 vertebra, psoas muscle, S1, S2 and S3 were statistically significant among the four groups ($P < 0.001$). The FF values of L3 vertebra and the pancreatic tail had the higher diagnostic efficacy when assessing the presence and extent of impaired glucose tolerance, respectively. For each percentile increased in the FF value of the L3 vertebra, the risk of diabetes entering the next stage increases 16%. Different organs in the abdomen have different sensitivity to fat deposition. The liver and pancreas have uneven distribution of fat deposits in people with different glucose tolerance. However, ectopic fat deposition do not change significantly with the duration of the disease. The FF value of L3 vertebra is a sensitive imaging index in patients with different glucose tolerance.

Keywords mDixon Quant, Magnetic resonance imaging, Ectopic fat deposition, Type 2 diabetes mellitus, Impaired glucose regulation

With the acceleration of urbanization and population aging, Type 2 diabetes mellitus (T2DM) is developing at an alarming rate around the world¹. Increased obesity is a strong risk factor for diabetes². Fatty acids produced by the body are mainly stored in adipose tissue in the form of triglycerides (TG). This is reversible initially, but eventually becomes permanent³. Subcutaneous adipose tissue (SAT) is the main site of excess TG storage, and its energy expenditure is limited⁴. When the SAT cannot store too much energy, too high TG can lead to the accumulation of TG in visceral adipose tissue (VAT), preperitoneal adipose tissue (pPAT), and non-adipose tissues such as the heart, liver, pancreas, and skeletal muscle⁵. These fat depots have been described as “ectopic fat depots”^{6,7}. Storage of ectopic and visceral fat may be associated with insulin resistance (IR), which is known

¹School of Medical, Nankai University, Nankai District, Tianjin, China. ²Department of Radiology, Tianjin First Central Hospital, 24 Fukang Road, Nankai District, Tianjin 300190, China. ³The First Central Clinical School, Tianjin Medical University, Nankai District, Tianjin, China. ⁴Department of Nephrology, Tianjin Fourth Central Hospital, 1 Zhongshan Road, Hebei District, Tianjin 300140, China. ⁵Bingshuo Yuan and Zhengzheng Tao have contributed equally to this work. ✉email: chuzhiq@aliyun.com; jiqianq@aliyun.com

to be the strongest predictor of the onset of diabetes⁸. Fat deposits in liver and skeletal muscle can induce IR and elevated blood glucose levels, which in turn may lead to T2DM⁹.

Excessive VAT and increased ectopic fat deposits contribute to IR¹⁰. Therefore, quantifying the deposition of ectopic fat in different organs and/or tissue is crucial for studying diabetes¹¹. However, the use of CT in measuring fat deposits is largely limited by the cumulative ionising radiation dose per subject, while MRI provides noninvasive high resolution imaging to investigate the abdominal tissue^{12,13}. MRI allows accurate assessment of whole body adipose tissue, including accurate assessment of fat in all organs¹⁴. Magnetic resonance spectroscopy (MRS) is being used for quantification of ectopic fat in parenchymal tissue and for characterization of fat (e.g. regarding composition in respect of saturated/unsaturated fatty acids) worldwide. However, due to the lack of specificity of MRS metabolite detection and high technical requirements for operators, MRS may not be suitable for screening asymptomatic patients^{15–17}. Using multi-echo imaging methods with a smaller flip angle, mDixon Quant achieves a proton density map that is closer to the true state. This technique calculates the T2* and R2* relaxation rates of tissues¹⁸. The computational model also accounts for lipids beyond triglycerides, ensuring that the fat ratio is not affected by field strength or other factors¹⁹. This non-invasive approach allows accurate fat quantification of internal organs.

To date, studies and analyses on T2DM fat quantification both domestically and internationally^{20–22} have mostly focused on single organs or a few organs, with inconsistent conclusions, which hinders a comprehensive comparison of the impact of blood glucose levels on abdominal fat deposition. The subjects included were also mostly limited to comparing normal volunteers and T2DM patients, with less attention paid to earlier-stage patients, and further refinement is needed for distinguishing different stages of T2DM.

In this study, mDixon Quant MRI was used to analyze the characteristic of abdominal ectopic fat deposition in people with different glucose tolerance quantitatively, and to explore the relationship between the progression of T2DM and abdominal ectopic fat deposition, and provide new ideas for diabetes prevention and treatment.

Materials and methods

Participants

In this study, 98 patients with different glucose tolerance in our hospital were retrospectively collected. The inclusion criteria were as follows: Ages were among 25 and 70 years old without MRI contraindication; MRI image quality was stable and good; meet the standards of medical care for T2DM in China 2020²³. The exclusion criteria were as follows: People with other types of diabetes or a history of taking nephrotoxic drugs; with acute or chronic hepatic disease caused by multiple etiologies exclude MASLD; with acute or chronic renal disease caused by multiple etiologies; acute or chronic pancreatitis; pregnant or lactating women; people who had fractures within 3 months, received radiation therapy within 1 month, and recently taken drugs that affect bone density; patients with poor cooperation or poor MRI image quality. The patients were stratified as impaired glucose tolerance (IGT) group (n = 18), the duration of diabetes less than 5 years (DMa group, n = 31) and longer than 5 years (DMb group, n = 49).

In addition, 38 healthy volunteers matched by sex and age were included as control group. The inclusion criteria were as follows: Ages were among 25 and 70 years old without MRI contraindication; No diabetes, hypertension, no history of chronic liver, pancreatic or kidney disease, and the blood glucose test in the past year was normal. The exclusion criteria were same as the patients. All subjects signed informed consents form prior to participation in the study and cooperated in the completion of abdominal imaging.

For patients, fasting venous blood was collected within one week prior to MRI. Serum creatinine (Scr), fasting blood glucose (FBG), glycosylated hemoglobin (HbA1c), triglyceride (TG), cholesterol (CHOL), low density lipoprotein cholesterol (LDL-C), high density lipoprotein cholesterol (HDL-C) was evaluated from the blood samples. A 2-h oral glucose tolerance test was performed to measure blood glucose two hours after orally taking an aqueous solution of 75 g of anhydrous dextrose. At the same time, the subject's height, weight, BMI and other basic data were recorded.

This study strictly adheres to the Helsinki Declaration and relevant laws and regulations. This study has been reviewed and approved by the Ethics Committee of Tianjin First Central Hospital.

MRI examinations

An Ingenia 3.0 T MR (Philips Healthcare, Amsterdam, The Netherlands) scanner was used and the subjects were imaged in supine positions. The subjects fasted for 4–6 h before MR scanning. Routine axial T1WI, T2WI and mDixon Quant sequence were acquired.

The imaging parameters of the axial mDixon Quant sequence were as follows: TE1 = 11.04 ms; TE2 = 11.84 ms; TE3 = 12.64 ms; TE4 = 13.24 ms; TE5 = 14.04 ms; TE6 = 14.84 ms; TR = 6.00 ms; flip angle = 4°; FOV = 200 mm × 400 mm × 105 mm and slice thickness = 6 mm.

Post processing

The original MR images were processed using the Philips IPS workstation to generate pseudo-color maps. Two experienced radiologists (with 3 and 6 years in abdominal radiology) measured the FF values of left hepatic lobe, right hepatic lobe, whole liver, spleen, pancreatic head, pancreatic body, pancreatic tail, left and right kidney, L3 vertebra, psoas muscle at the level of L3 vertebra (hereinafter referred to as FF_{LL}, FF_{RL}, FF_{WL}, FF_{SP}, FF_{PH}, FF_{PB}, FF_{PT}, FF_{LK}, FF_{RK}, FF_{L3}, FF_{PM}) and the fat areas (S values) of the abdominal cavity. Due to the large volume of the liver and spleen, the volumes region of interest (VOIs) were delineated. Other organs were small, and regions of interests (ROIs) were placed in the layer. S values included the total fat area of the abdomen at the level of the L3 (S1), the internal abdominal fat area of organs (S2), and S3 referred to the ratio of S2 to S1 (Fig. 1).

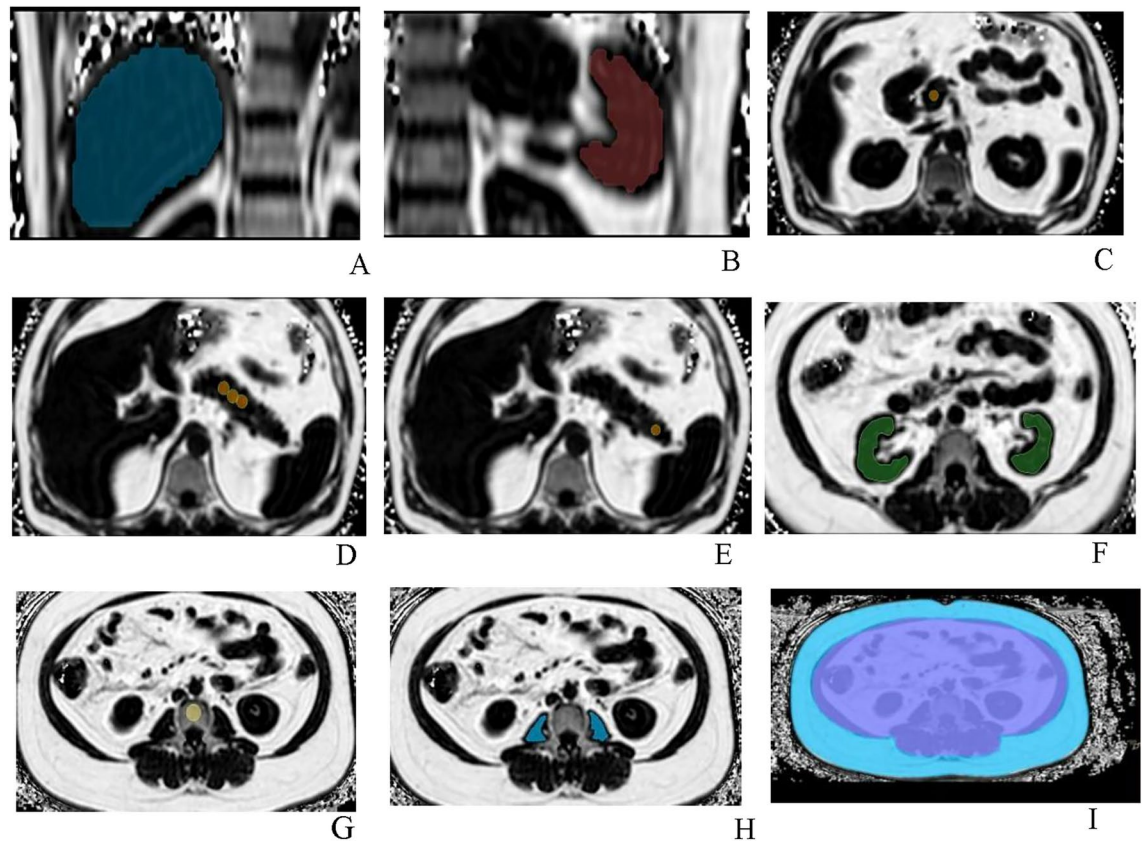


Fig. 1. Schematic diagram of VOI or ROI placement. (A) liver; (B) spleen; (C) pancreatic head; (D) pancreatic body; (E) pancreatic tail; (F) bilateral kidneys; (G) L3 vertebra; (H) bilateral psoas muscles; (I) within blue (including purple) was the S1 range, within purple was the S2 range.

Statistical analysis

All data were statistically analyzed using SPSS 25.0 software (SPSS, USA). The continuous data that conformed to the normal distribution were represented as mean \pm standard deviation ($\bar{x} \pm s$). The intraclass correlation (ICC) was used to compare the agreement among the FF values and S values measured by the two radiologists. One-way ANOVA was used to compare the FF_{LL} , FF_{RL} , FF_{WL} , FF_{PH} , FF_{PB} , FF_{PT} , FF_{L3} . The *t*-test of paired samples was used to compare the FF_{LK} , FF_{RK} , FF_{PM} . The differences in general clinical data among multiple groups were compared by chi-square test/one-way ANOVA and Welch ANOVA. Data that did not conform to the normal distribution were tested by nonparametric test. Pearson or Spearman correlation analysis was used to compare the correlation among the FF values, S values and biochemical indexes, and the correlation among each parameter. Receiver operating characteristic (ROC) curve analysis and ordered multivariate logistic regression were used to analyze the diagnostic value of FF values in patients with different glucose tolerance. $P < 0.05$ was considered statistically significant.

Results

Demographic characteristics and clinical outcomes

A total of 98 patients and 38 healthy volunteers were included in this study. There were significant differences in BMI and weight among four groups (all $P < 0.001$). The FBG, 2 h OGTT, HbA1c (%), Scr, BUN, AST, and ALT had significant differences among three patients groups (all $P < 0.05$). The results of the two-by-two comparison were shown in Table 1. The differences among other clinical indicators were not statically significant.

ICC analysis

FF_{LL} , FF_{RL} , FF_{WL} , FF_{SP} , FF_{PH} , FF_{PB} , FF_{PM} , S1, S2 had excellent interobserver agreement with ICCs of 0.886(0.809–0.932), 0.899(0.830–0.940), 0.817(0.709–0.887), 0.795(0.680–0.873), 0.908(0.788–0.962), 0.906(0.852–0.941), 0.802(0.694–0.875), 0.890(0.819–0.933), 0.781(0.638–0.872), respectively. The FF_{L3} and FF_{PT} displayed a moderate interobserver agreement with ICC of 0.742(0.575–0.809) and 0.732(0.683–0.891).

Intra-group comparison of FF value for the same organ

There were no significant differences in FF_{LL} , FF_{RL} , FF_{WL} , FF_{PH} , FF_{PB} , FF_{PT} in control group (all $P > 0.05$), while there were significant differences in IGT, DMA and DMb groups (all $P < 0.05$). There were no significant

| Projects | Control group (n = 38) | IGT group (n = 18) | DMa group (n = 31) | DMb group (n = 49) | Statistical value | P-value |
|--------------------------|---------------------------|-----------------------|----------------------------------|----------------------------------|-------------------|---------|
| Sex (male/female) | 22/16 | 9/9 | 23/8 | 38/11 | 4.963 χ^2 | 0.084 |
| Age (year) | 46 \pm 11 | 47 \pm 9 | 48 \pm 13 | 47 \pm 2 | 0.916 | 0.436 |
| Duration (year) | – | – | 1.31 \pm 0.59 | 11.86 \pm 1.76 | 52.933 | 0.000 |
| Height (m) | 168.61 \pm 1.30 | 165.54 \pm 2.06 | 170.00 \pm 4.70 | 174.81 \pm 1.64 | 2.154 | 0.101 |
| Weight (kg) | 66.98 \pm 1.90 | 70.80 \pm 2.92 | 89.00 \pm 4.39 ^{aΔb#} | 86.75 \pm 3.54 ^{aΔb#} | 13.728 | 0.000 |
| BMI (kg/m ²) | 23.50 \pm 0.52 | 25.20 \pm 1.38 | 28.26 \pm 0.91 ^{aΔ} | 29.01 \pm 0.70 ^{aΔ} | 14.748 | 0.000 |
| FBG (mmol/L) | – | 6.54 \pm 0.72 | 8.43 \pm 0.42 | 7.35 \pm 0.39 ^{b*} | 3.425 | 0.039 |
| 2hOGTT (mmol/L) | – | 8.54 \pm 0.46 | 15.14 \pm 1.88 ^{bΔ} | 16.32 \pm 0.92 ^{bΔ} | 35.840 | 0.000 |
| HbA1c (mmol/mol) | – | 6.28 \pm 0.34 | 10.18 \pm 0.66 ^{bΔ} | 8.50 \pm 0.48 ^{bΔc*} | 23.412 | 0.000 |
| Scr (μmol/L) | – | 60.06 \pm 2.99 | 68.43 \pm 5.64 ^{b*} | 72.46 \pm 6.16 | 5.735 | 0.007 |
| BUN (mmol/L) | – | 3.97 \pm 0.33 | 3.92 \pm 0.28 | 5.51 \pm 0.44 ^{c*} | 3.306 | 0.044 |
| TG (mmol/L) | – | 1.56 \pm 0.45 | 1.97 \pm 0.63 | 3.08 \pm 0.54 | 1.294 | 0.282 |
| CHOL (mmol/L) | – | 5.13 \pm 0.53 | 5.71 \pm 0.29 | 5.72 \pm 0.24 | 0.580 | 0.564 |
| HDL-C (mmol/L) | – | 1.33 \pm 0.12 | 1.22 \pm 0.13 | 1.14 \pm 0.08 | 1.559 | 0.219 |
| LDL-C (mmol/L) | – | 3.38 \pm 0.40 | 3.84 \pm 0.18 | 3.84 \pm 0.19 | 0.760 | 0.473 |
| ALT(u/L) | – | 20.91 \pm 2.03 | 23.63 \pm 2.95 | 42.82 \pm 9.41 ^{b*} | 4.440 | 0.020 |
| AST (u/L) | – | 20.29 \pm 1.57 | 24.21 \pm 3.87 | 36.43 \pm 7.27 ^{b*} | 5.190 | 0.010 |

Table 1. Comparative results of demographic and anthropometric indicators. # $P < 0.01$; * $P < 0.05$; $\Delta P < 0.001$. –: no data; a: compared to the control group; b compared to the IGT group. Z indicates that a nonparametric test was used, and the corresponding statistic was Z value; χ^2 indicates that the chi-square test was used, and the corresponding statistic was the chi-square value. BMI Body mass index; FBG Fasting blood glucose; 2 h OGTT: 2 h oral glucose tolerance test; HbA1c Glycosylated hemoglobin; TG Triglyceride; CHOL Cholesterol; HDL-C High density lipoprotein cholesterol; LDL-C Low density lipoprotein cholesterol.

differences in FF_{LK}, FF_{RK} and FF_{PM} in all of the groups (all $P > 0.05$), so we took the two-sided average as the final value (Table 2).

Inter-group comparison of FF values for different organs and S values

Except kidney ($P = 0.546$), the overall differences in FF values among multiple groups were statistically significant (all $P < 0.05$) (Table 2). The overall differences of S1, S2 and S3 among four groups were statistically significant (all $P < 0.001$). The results of further pair-by-two comparisons were as Fig. 2.

Correlation of FF values, S values and clinical indicators

FF_{LL} ($r = 0.317$, $P = 0.018$), FF_{RL} ($r = 0.374$, $P = 0.005$), FF_{WL} ($r = 0.366$, $P = 0.006$) and HbA1c were positively correlated. FF_{PH} ($r = -0.442$, $P = 0.024$) and FF_{PB} ($r = -0.389$, $P = 0.031$) were negatively correlated with ALT. FF_{PT} and LDL-C were positively correlated ($r = 0.406$, $P = 0.029$). FF_{L3} and ALT ($r = 0.450$, $P = 0.005$), FBG ($r = 0.356$, $P = 0.032$) were positively correlated. However, the correlations for each group were weak (Table 3, Fig. 3).

ROC curves for the diagnostic performance of MR parameters

(1) For the control group and IGT group: The AUCs of FF_{LL}, FF_{RL}, FF_{Sp}, FF_{PH} and FF_{L3} were 0.690, 0.689, 0.709, 0.703, and 0.720, respectively, all showing statistical differences ($P < 0.05$), with the AUC corresponding to the FF value of the L3 vertebra being the highest. (2) For the control group and T2DM group: The AUCs of FF_{LL}, FF_{RL}, FF_{WL}, FF_{Sp}, FF_{PB}, FF_{PT}, FF_{L3} and FF_{PM} were 0.797, 0.809, 0.799, 0.689, 0.866, 0.855, 0.885, and 0.755, respectively, all showing statistical differences ($P < 0.05$), with the AUC corresponding to the FF_{L3} being the highest. (3) For the IGT group and T2DM group: The AUCs of FF_{PH}, FF_{PB}, FF_{PT}, FF_{L3} were 0.727, 0.796, 0.828, and 0.751, respectively, all showing statistical differences ($P < 0.05$), with the AUC corresponding to the FF_{PT} being the highest (Fig. 4).

Ordered logistic regression analysis

According to the results of the inter-group analysis mentioned earlier, multiple factors with differences between groups were used as independent variables for univariate ordered multiple logistic regression analysis. Since there was a statistically significant difference in BMI and weight across groups, they were included and adjusted during the analysis. The results showed that FF_{LL}, FF_{RL}, FF_{WL}, FF_{Sp}, FF_{PB}, FF_{PT} and FF_{L3} were associated with different glucose tolerance stages ($P < 0.05$). Multivariate ordered multiple logistic regression was performed on the above influencing factors, and the results indicated that FF_{L3} was an independent risk factor for different glucose tolerance stages ($P < 0.05$) (Table 4). For every one percentage point increase in FF_{L3}, the risk of diabetes entering the next stage increased by EXP (0.390) = 1.16 times. That is, if a pre-diabetic patient's FF_{L3} increased from 55 to 56%, the risk of diabetes would increase by 1.16 times.

| | Control group | IGT group | DMa group | DMb group | F | P |
|--|-----------------|--------------|--------------|------------------|--------|-------|
| FF _{LL} | 3.10(2.88,3.78) | 6.08 ± 0.82 | 6.85 ± 0.68 | 9.12(7.67,11.40) | 22.347 | 0.000 |
| FF _{RL} | 2.05(1.69,2.65) | 5.44 ± 1.00 | 5.82 ± 0.72 | 8.21(6.67,10.45) | 22.166 | 0.000 |
| FF _{WL} | 2.15(2.14,3.05) | 5.55 ± 0.93 | 6.37 ± 0.72 | 8.46(6.93,10.71) | 22.246 | 0.000 |
| F | 0.774 | 7.284 | 6.439 | 4.442 | – | – |
| P | 0.701 | 0.001 | 0.004 | 0.019 | – | – |
| FF _{Sp} | 0.53(0.44,0.67) | 1.13 ± 0.42 | 2.60 ± 0.46 | 0.95(0.78,1.23) | 9.723 | 0.000 |
| FF _{PH} | 6.64 ± 0.52 | 7.75 ± 0.85 | 12.02 ± 1.04 | 14.17 ± 0.79 | 19.179 | 0.000 |
| FF _{PB} | 6.02 ± 0.35 | 7.01 ± 0.72 | 10.09 ± 0.76 | 12.86 ± 0.89 | 14.032 | 0.000 |
| FF _{PT} | 6.56 ± 0.42 | 7.68 ± 0.55 | 10.74 ± 0.79 | 13.24 ± 1.15 | 15.470 | 0.000 |
| F | 0.647 | 3.427 | 3.966 | 3.723 | – | – |
| P | 0.526 | 0.043 | 0.031 | 0.037 | – | – |
| FF _{LK} | 6.44 ± 0.25 | 6.01 ± 0.42 | 5.77 ± 0.34 | 7.27 ± 1.07 | 0.713 | 0.546 |
| FF _{RK} | 6.14 ± 0.29 | 6.07 ± 0.38 | 5.70 ± 0.40 | 7.01 ± 1.02 | | |
| t | 1.638 | – 0.848 | 0.298 | 1.279 | – | – |
| P | 0.110 | 0.408 | 0.768 | 0.207 | – | – |
| FF _{L3} | 39.29 ± 1.75 | 46.21 ± 1.80 | 50.21 ± 1.80 | 54.45 ± 0.98 | 21.869 | 0.000 |
| FF _{left PM} | 4.15 ± 0.36 | 4.67 ± 0.55 | 5.30 ± 0.53 | 6.11 ± 1.27 | 7.451 | 0.000 |
| FF _{right PM} | 3.97 ± 0.33 | 4.92 ± 0.61 | 4.91 ± 0.48 | 6.30 ± 1.28 | | |
| t | – 0.997 | – 0.756 | – 1.815 | – 1.868 | – | – |
| P | 0.325 | 0.460 | 0.084 | 0.070 | – | – |
| S1 (× 10 ³ mm ²) | 51.29 ± 1.91 | 57.43 ± 3.32 | 62.82 ± 4.81 | 68.68 ± 17.47 | 14.709 | 0.000 |
| S2 (× 10 ³ mm ²) | 20.42 ± 1.05 | 22.94 ± 2.16 | 27.82 ± 2.16 | 32.16 ± 1.07 | 12.256 | 0.000 |
| S3(%) | 39.38 ± 0.85 | 39.43 ± 1.9 | 44.74 ± 1.05 | 46.89 ± 1.02 | 12.386 | 0.000 |

Table 2. Intra-group and inter-group comparison of FF values and S values. FF_{LL}: FF values of left hepatic lobe; FF_{RL}: FF values of right hepatic lobe; FF_{WL}: FF values of whole liver; FF_{Sp}: FF values of spleen; FF_{PH}: FF values of pancreatic head; FF_{PB}: FF values of pancreatic body; FF_{PT}: FF values of pancreatic tail; FF_{LK}: FF values of left kidney; FF_{RK}: FF values of right kidney; FF_{L3}: FF values of L3 vertebra body; FF_{PM}: FF values of psoas muscle at the level of L3; S1: S values included the total fat area of the abdomen at the level of the L3; S2: the internal abdominal fat area of organs; S3: the ratio of S2 to S1.

Discussion

mDixon Quant MRI provides a non-invasive, accurate and comprehensive assessment of fat content with short scanning times and convenience to operate²⁴. Some clinical studies^{25–27} have reported quantitative assessment of abdominal fat deposits in diabetes using MRI. But most of them were single organ studies or included only patients with confirmed diagnosis of diabetes as subjects. In our study, abdominal ectopic fat deposition begins at the IGT stage and is unevenly distributed in the liver and pancreas; however, ectopic fat deposition does not significantly change with the duration of T2DM and FF_{L3} is a sensitive imaging index in patients with different glucose tolerance, which has not been reported in previous studies.

Both the liver and the pancreas are crucial organs in blood glucose regulation. The breakdown of the dynamic equilibrium of blood glucose not only signals abnormal organ function but also further intensifies the abnormal glycolipid metabolism in these organs, eventually resulting in IR. By employing mDixon Quant MRI, our study reveals that in IGT stage, the liver and the pancreas have already exhibited remarkable alterations in fat distribution, and the distribution pattern presents certain characteristics. This is similar to previous studies^{28,29}, which have shown that abdominal fat deposition begins in the pre-diabetic stage and is unevenly distributed in the liver and pancreas.

Our study found that FF_{LL}, FF_{RL}, FF_{WL} were significantly different among multiple groups. This result was consistent with several clinical studies^{26,30}. Due to poor blood glucose control, patients are prone to fat deposition in the liver, leading to fatty liver. At the same time, fatty liver patients, due to IR, face even greater difficulties in blood glucose control, thereby increasing the risk of developing diabetes. With the development of diabetes, we found fat deposition in the left hepatic lobe was more obvious, which was contrary to the study of Capitan³¹, they found fat deposition were more pronounced in right hepatic lobe than in left. Whatever it demonstrated that the deposition of fatty liver is uneven. As for different results, there were two possible reasons, one was the selection of the ROI. The 3D volume outline in our study was more accurate compared to Capitan's 2D ROI. Secondly, it could be that the participants were ethnically diverse and there were some dietary differences.

Similarly, the fat deposition in the pancreas is also non-uniform. Fat deposition was more obvious in pancreatic head and tail than in pancreatic body in patients groups, which was consistent with Chai et al.³² and Zeng et al.³³, suggesting an uneven distribution of pancreatic fat in IGT and T2DM. This might be strongly related to the uneven distribution of β cells in the pancreas. In addition, the ROC curve analysis showed that FF_{PT}

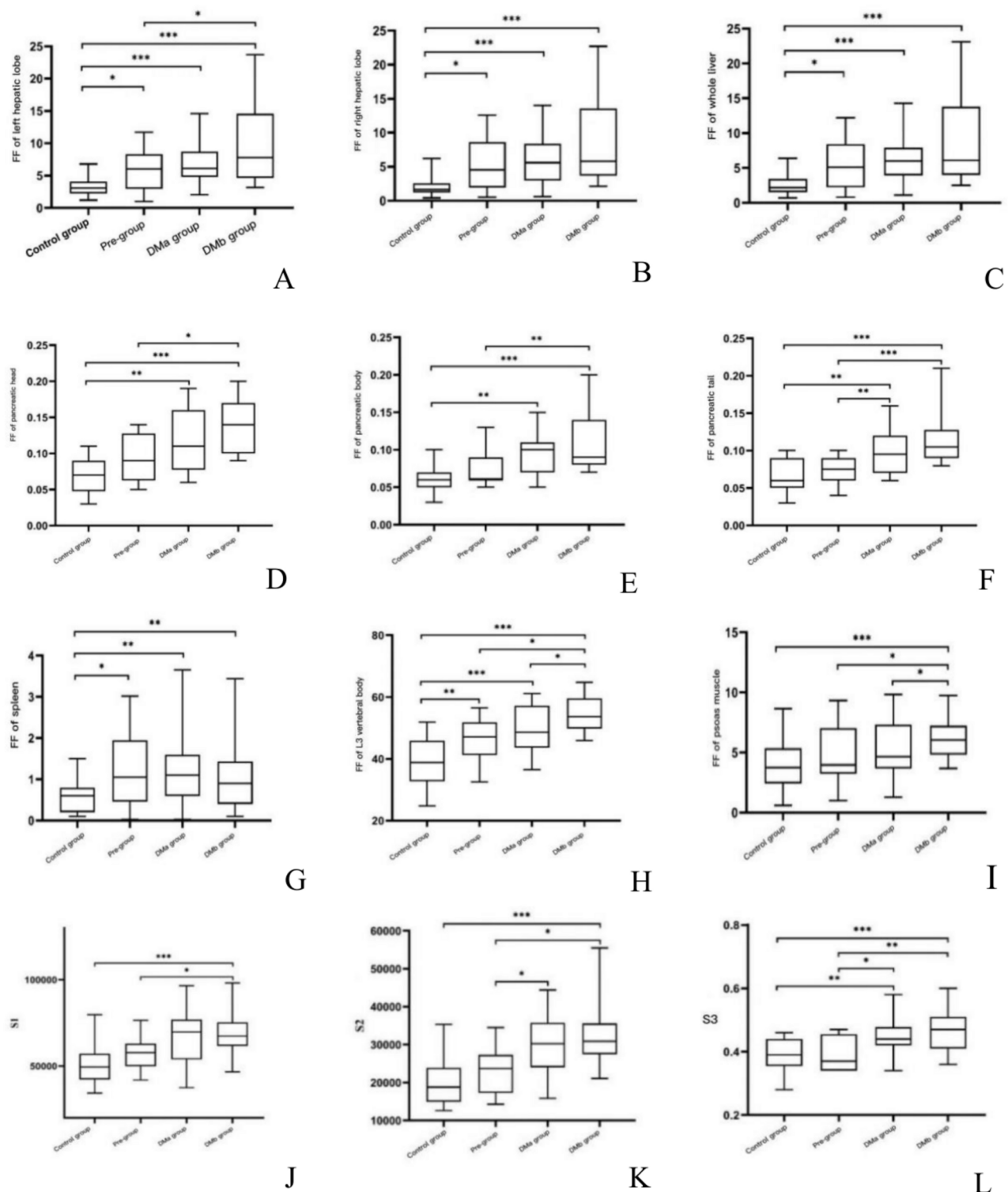


Fig. 2. The (A–I) plots were FF_{LL} , FF_{RL} , FF_{WL} , FF_{PH} , FF_{PB} , FF_{PT} , FF_{Sp} , FF_{L3} , FF_{PM} . The (J–L) plots were the results of further pair-by-two comparisons of S1, S2 and S3. * $P < 0.05$, ** $P < 0.01$, *** $P < 0.001$.

had the best effect on assessing the degree of impaired glucose tolerance. This suggested that fat deposition had a more significant effect on pancreatic tail during the progression of diabetes. Although pancreatic fat deposition might be a potential cause of T2DM, the relationship between IR and lipid metabolism disorders remained to be further investigated and discussed. We found that FF_{PH} , FF_{PB} were associated with ALT and FF_{PT} was associated with LDL-C. This suggested that there might be a potential link between fat changes occurred in different parts of the pancreas and reduced liver function.

| | FPG (mmol/L) | 2 h OGTT (mmol/L) | HbA1c (%) | TG (mmol/L) | CHOL (mmol/L) | HDL-C (mmol/L) | LDL-C (mmol/L) | Scr (umol/L) | AST | ALT | BUN (mmol/L) |
|------------------|------------------|----------------------|-------------------|------------------|------------------|----------------|-------------------|---------------|------------------|----------------|------------------|
| FF | r, P | r, P | r, P | r, P | r, P | r, P | r, P | r, P | r, P | r, P | r, P |
| FF _{LL} | 0.047, 0.739 | -0.084, 0.563 | 0.317*, 0.018 | -0.061, 0.670 | -0.106, 0.468 | -0.019, 0.893 | -0.009, 0.951 | -0.065, 0.654 | -0.089, 0.532 | 0.214, 0.144 | -0.002, 0.990 |
| FF _{RL} | 0.000, 0.998 | -0.102, 0.479 | 0.374**, 0.005 | -0.046, 0.745 | -0.065, 0.655 | -0.041, 0.775 | 0.052, 0.730 | -0.074, 0.609 | -0.080, 0.578 | 0.205, 0.162 | 0.021, 0.885 |
| FF _{WL} | -0.015, 0.913 | -0.063, 0.663 | 0.366*, 0.006 | -0.088, 0.533 | -0.055, 0.707 | 0.005, 0.969 | 0.068, 0.652 | -0.086, 0.552 | -0.115, 0.423 | 0.126, 0.394 | 0.042, 0.772 |
| FF _{Sp} | 0.105, 0.422 | -0.184, 0.172 | -0.107, 0.408 | -0.158, 0.231 | 0.034, 0.803 | 0.199, 0.135 | 0.159, 0.264 | -0.100, 0.459 | -0.105, 0.433 | -0.037, -0.790 | 0.021, 0.885 |
| FF _{PH} | 0.223, 0.246 | 0.191, 0.340 | -0.215, 0.245 | 0.123, 0.526 | 0.436*, 0.021 | 0.033, 0.864 | 0.345, 0.098 | 0.082, 0.553 | -0.193, 0.325 | -0.442*, 0.024 | 0.092, 0.641 |
| FF _{PB} | 0.128, 0.492 | 0.184, 0.331 | -0.012, 0.946 | 0.129, 0.468 | 0.300, 0.095 | 0.106, 0.550 | 0.329, 0.071 | 0.020, 0.910 | -0.163, 0.366 | -0.389*, 0.031 | 0.083, 0.653 |
| FF _{PT} | 0.076, 0.671 | 0.236, 0.201 | 0.041, 0.819 | 0.083, 0.647 | 0.261, 0.164 | -0.025, 0.888 | 0.406*, 0.029 | -0.048, 0.792 | -0.104, 0.566 | -0.218, 0.230 | -0.087, 0.636 |
| FF _{L3} | 0.356*, 0.032 | 0.214, 0.184 | 0.286, 0.063 | 0.123, 0.444 | -0.081, 0.628 | -0.419*, 0.007 | -0.089, 0.618 | -0.196, 0.219 | 0.181, 0.263 | 0.450*, 0.005 | -0.219, 0.175 |
| FF _{PM} | -0.003, 0.982 | -0.137, 0.360 | 0.019, 0.896 | -0.083, 0.567 | -0.013, 0.932 | 0.004, 0.979 | -0.109, 0.477 | 0.099, 0.507 | -0.072, 0.630 | -0.001, 0.994 | 0.038, 0.804 |
| S1 | 0.239, 0.118 | 0.048, 0.758 | 0.117, 0.430 | 0.009, 0.954 | -0.106, 0.495 | -0.161, 0.286 | -0.161, 0.321 | -0.068, 0.663 | 0.111, 0.480 | 0.011, 0.947 | -0.228, 0.136 |
| S2 | 0.091, 0.559 | -0.033, 0.360 | 0.071, 0.631 | 0.052, 0.727 | -0.070, 0.649 | -0.161, 0.285 | -0.140, 0.389 | 0.033, 0.829 | 0.179, 0.251 | 0.056, 0.733 | -0.055, 0.723 |
| S3 | -0.224, 0.144 | 0.214, 0.184 | -0.017, 0.909 | 0.104, 0.486 | 0.064, 0.679 | -0.047, 0.755 | 0.036, 0.825 | 0.148, 0.336 | 0.157, 0.316 | 0.014, 0.933 | 0.204, 0.183 |

Table 3. Correlation analysis of FF values and S values of each organ and clinical indexes. *The two parameters of the corresponding row and column were related. FF_{LL}: FF values of left hepatic lobe; FF_{RL}: FF values of right hepatic lobe; FF_{WL}: FF values of whole liver; FF_{Sp}: FF values of spleen; FF_{PH}: FF values of pancreatic head; FF_{PB}: FF values of pancreatic body; FF_{PT}: FF values of pancreatic tail; FF_{PM}: FF values of psoas muscle at the level of L3; S1: S values included the total fat area of the abdomen at the level of the L3; S2: the internal abdominal fat area of organs; S3: the ratio of S2 to S1.

Spleen plays an important role in immune system, but the mechanism how fat deposition affects the spleen is not clear. Obesity has been found to be associated with immune disorders, which in turn can accelerates fat deposition in many organs³⁴. Our study confirmed that fat deposition have occurred in spleen in the early stage of diabetes and persist during the disease. Wang et al.³⁵ also noted that increased level of inflammation caused by T2DM could cause spleen damage. Since the spleen, as an important immune organ of the human body, is responsible for filtering pathogens and senescent red blood cells in the blood. When the spleen is affected by inflammation, its normal functions may be compromised, and it is likely to manifest as fat deposition.

It is worth noting that we have discovered that FF_{L3} was a significant influencing factor among patients with different glucose tolerances and is likely a potential predictor. Based on the current results, for every one-percentile increase in FF_{L3}, the risk of diabetes progressing to the next stage increases by 16%. It can be seen that the vertebral bodies are highly sensitive to different glucose tolerance levels. Studies^{36,37} have demonstrated that within the bone marrow microenvironment, there exists an extremely complex and intricate signaling communication mechanism among bone marrow adipocytes, osteoblasts, osteoclasts, and various other cell types. However, in a hyperglycemic environment, this homeostasis is disrupted. Hyperglycemia can significantly affect the differentiation fate of bone marrow mesenchymal stem cells. It induces these cells to differentiate more towards the adipocyte lineage while inhibiting their differentiation process towards osteoblasts. This abnormal differentiation process ultimately leads to a significant increase in the number of adipocytes in the bone marrow and a decrease in the number of osteogenic- function-bearing cells. Consequently, the fat content has increased significantly. Meanwhile, in the paravertebral muscles, which serve to protect the vertebral bodies, the fat content showed the same trend of change, which was similar to the findings of Kiefer³⁸. The location of IMAT in skeletal muscle appears to be an important determinant of IR³⁹, but we found that fat deposition in paravertebral muscle was relatively low, and sensitivity of paravertebral muscle was poor compared with other parts. This may be related to the changes in the composition of the vertebral bodies.

Abdominal fat is also an important site of diabetic ectopic fat deposition⁴⁰. Most patients with diabetes are central obese. The definition of central obesity is mostly based on waist circumference⁴¹. In clinical studies, BMI as basic physical information does not reflect the fat accumulation in the internal abdominal cavity, so imaging-based evaluation is increasingly accepted^{33,42}. In our study, subcutaneous and visceral fat area at the level of the L3 were included. To reduce individual differences, the proportion of visceral fat area in abdominal area was compared as a new parameter. Our result suggested an increase in abdominal fat area was beneficial for the diagnosis of T2DM. This was similar with the study by Chen et al.⁴³. It is widely acknowledged that abdominal obesity constitutes a pivotal element of metabolic syndrome. To a certain degree, abdominal obesity frequently exhibits an association with IR.

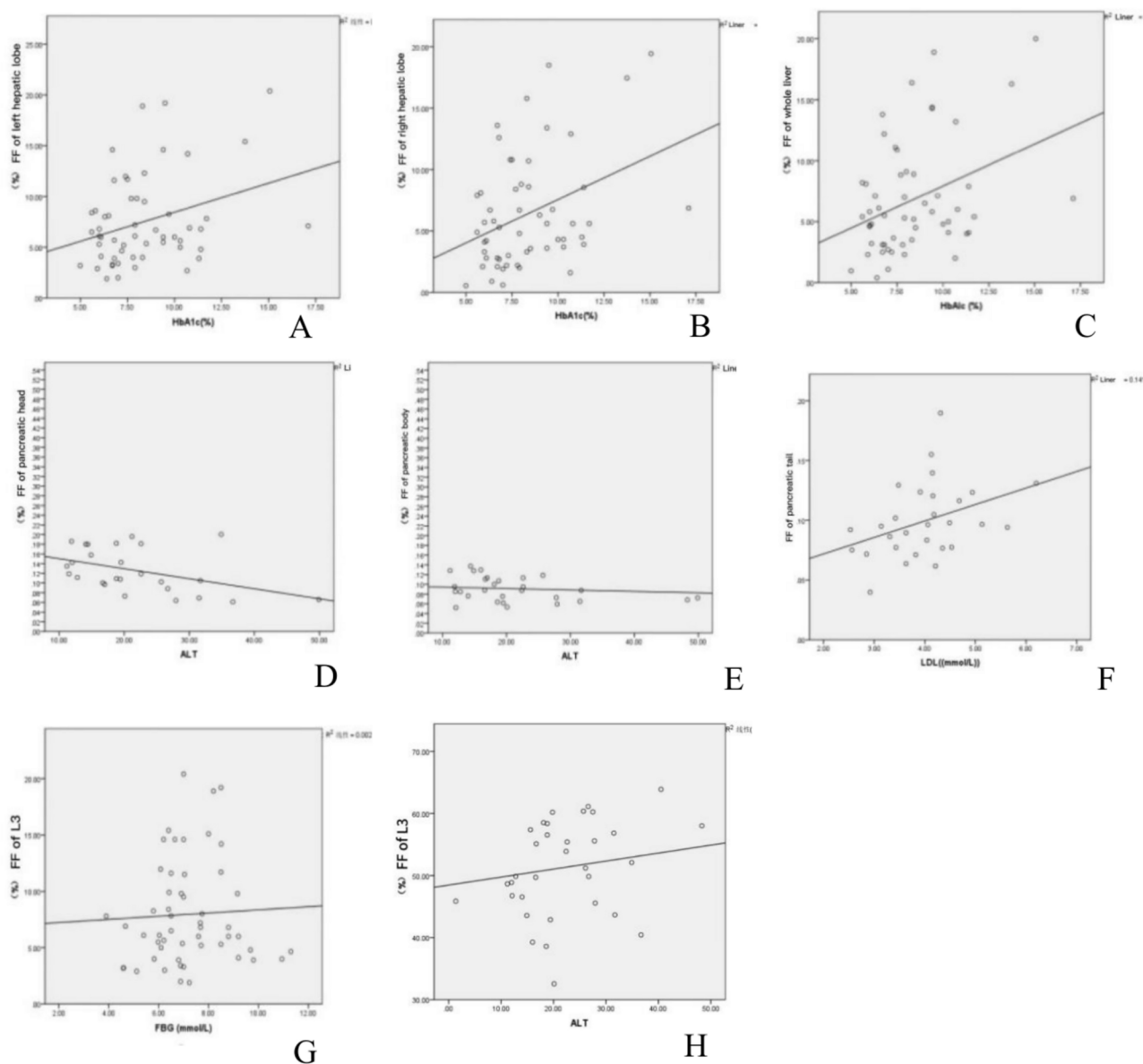


Fig. 3. Pearson or Spearman correlation analysis diagrams. (A–C) were the scatterplots of FF_{LL}, FF_{RL}, FF_{WL} and HbA1c; (D–E) were the scatterplot of FF_{PH}, FF_{PB} and ALT; (F) was the scatterplot of the correlation between FF_{PT} and LDL-C. (G–H) were the associated scatter of FF_{L3} and FBG, ALT.

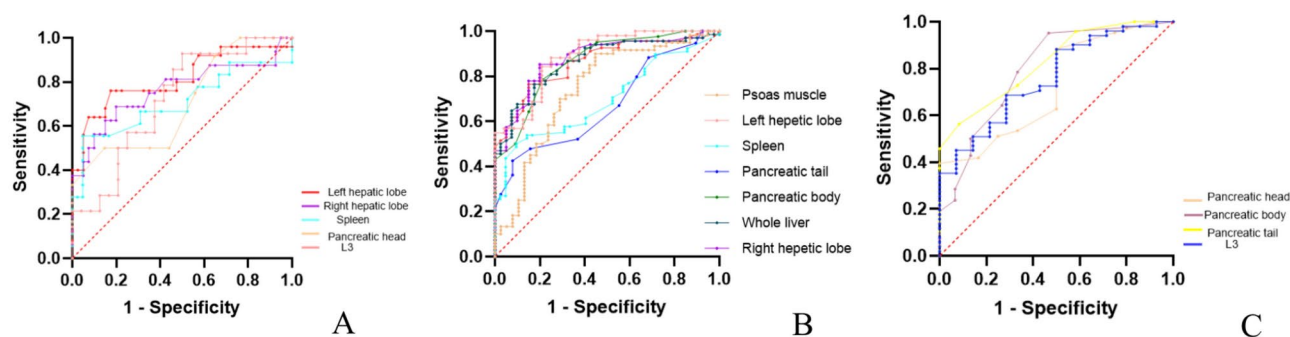


Fig. 4. ROC curve analysis. (A) Between the control group and IGT group; (B) between the control group and T2DM group; (C) between the IGT group and T2DM group.

| | Parallelism test | Single factor | | | Multiple factor | | |
|------------------|------------------|---------------|-------------------------|-------------|-----------------|-------------------------|-------------|
| | | P | 95% confidence interval | | P | 95% confidence interval | |
| | | | Lower limit | Upper limit | | Lower limit | Upper limit |
| FF _{LL} | 0.186 | 0.003 | 0.212 | 1.070 | 0.717 | −0.714 | 1.039 |
| FF _{RL} | 0.216 | 0.002 | 0.192 | 0.849 | 0.462 | −0.425 | 0.934 |
| FF _{WL} | 0.117 | 0.004 | 0.175 | 0.892 | 0.446 | −0.622 | 0.274 |
| FF _{Sp} | 0.388 | 0.065 | 0.068 | 2.264 | 0.194 | −3.968 | 0.804 |
| FF _{PH} | 0.001 | – | – | – | – | – | – |
| FF _{PB} | 0.108 | 0.010 | 17.496 | 131.422 | 0.074 | −5.869 | 127.518 |
| FF _{PT} | 0.071 | 0.022 | 13.643 | 173.728 | 0.700 | −54.297 | 80.906 |
| S1 | 0.001 | – | – | – | – | – | – |
| S2 | 0.001 | – | – | – | – | – | – |
| S3 | 0.001 | – | – | – | – | – | – |
| FF _{PM} | 0.006 | – | – | – | – | – | – |
| FF _{L3} | 0.889 | 0.019 | 0.064 | 0.716 | 0.039 | 0.006 | 0.227 |

Table 4. Ordered logistic regression analysis results. FF_{LL}: FF values of left hepatic lobe; FF_{RL}: FF values of right hepatic lobe; FF_{WL}: FF values of whole liver; FF_{Sp}: FF values of spleen; FF_{PH}: FF values of pancreatic head; FF_{PB}: FF values of pancreatic body; FF_{PT}: FF values of pancreatic tail; FF_{L3}: FF values of L3 vertebra body; FF_{PM}: FF values of psoas muscle at the level of L3; S1: S values included the total fat area of the abdomen at the level of the L3.

The study had certain limitations. Firstly, the sample size is relatively small, especially for IGT patients. In the future, we will further expand the sample size and try to include multicenter data to confirm our preliminary conclusions. Secondly, this study is a cross-sectional study, and further longitudinal follow-up data will be collected to observe the relationship between T2DM progression and abdominal fat deposition. Thirdly, we measured “internal abdominal fat area” instead of visceral adipose tissue that does not include organs within the abdominal cavity in our study. In the future we will collect data to do more in-depth studies on visceral adipose tissue, such as perirenal and renal sinus fat tissue.

In conclusion, Different organs in the abdomen have different sensitivity to fat deposition. The liver and pancreas have uneven distribution of fat deposits in people with different glucose tolerance. However, ectopic fat deposition do not change significantly with the duration of the disease. The FF value of L3 is a sensitive imaging index in patients with different glucose tolerance.

Data availability

The datasets used and/or analysed during the current study available from the corresponding author on reasonable request.

Received: 7 August 2024; Accepted: 25 February 2025

Published online: 01 March 2025

References

- Antza, C., Kostopoulos, G., Mostafa, S., Nirantharakumar, K. & Tahrani, A. The links between sleep duration, obesity and type 2 diabetes mellitus. *J. Endocrinol.* **252**, 125–141. <https://doi.org/10.1530/JOE-21-0155> (2022).
- Ng, A. C. T., Delgado, V., Borlaug, B. A. & Bax, J. J. Diabetes: The combined burden of obesity and diabetes on heart disease and the role of imaging. *Nat. Rev. Cardiol.* **18**, 291–304. <https://doi.org/10.1038/s41569-020-00465-5> (2021).
- Taylor, R. Pathogenesis of type 2 diabetes: Tracing the reverse route from cure to cause. *Diabetologia* **51**, 1781–1789. <https://doi.org/10.1007/s00125-008-1116-7> (2008).
- Ibrahim, M. M. Subcutaneous and visceral adipose tissue: Structural and functional differences. *Obes. Rev.* **11**, 11–18. <https://doi.org/10.1111/j.1467-789X.2009.00625.x> (2010).
- Piché, M., Tchernof, A. & Després, J. Obesity phenotypes, diabetes, and cardiovascular diseases. *Circ. Res.* **126**, 1477–1500. <https://doi.org/10.1161/CIRCRESAHA.119.315901> (2020).
- Zhang, Q. et al. Magnetic resonance imaging assessment of abdominal ectopic fat deposition in correlation with cardiometabolic risk factors. *Front. Endocrinol.* <https://doi.org/10.3389/fendo.2022.820023> (2022).
- Cao, M. et al. Quantification of ectopic fat storage in the liver and pancreas using six-point dixon MRI and its association with insulin sensitivity and B-cell function in patients with central obesity. *Eur. Radiol.* <https://doi.org/10.1007/s00339-022-06265-4> (2023).
- Ndisang, J. F., Vannacci, A. & Rastogi, S. Insulin resistance, type 1 and type 2 diabetes, and related complications 2017. *J. Diabetes Res.* <https://doi.org/10.1155/2017/6473538> (2017).
- Larson-Meyer, D. E. et al. Intrahepatic and intramyocellular lipids are determinants of insulin resistance in prepubertal children. *Diabetologia* **54**, 869–875. <https://doi.org/10.1007/s00125-011-2070-5> (2011).
- Chait, A. & den Hartigh, L. J. Adipose tissue distribution inflammation and its metabolic consequences including diabetes and cardiovascular disease. *Front. Cardiovasc. Med.* <https://doi.org/10.3389/fcvm.2020.00142> (2020).
- Yu, X., Huang, Y., Feng, Y., Cheng, Z. & Cai, X. Well-controlled versus poorly controlled diabetes in patients with obesity: Differences in MRI-evaluated pancreatic fat content. *Quant. Imaging Med. Surg.* **13**, 3496–3507. <https://doi.org/10.2103/qims.2023.3496> (2023).

12. Lin, D. et al. Automated measurement of pancreatic fat deposition on dixon MRI using Nnu-net. *J. Magn. Reson. Imaging*. **57**, 296–307. <https://doi.org/10.1002/jmri.27759> (2023).
13. Schwenzer, N. F. et al. Quantification of pancreatic lipomatosis and liver steatosis by MRI: Comparison of in/opposed-phase and spectral-spatial excitation techniques. *Invest. Radiol.* **43**, 330–337. <https://doi.org/10.1097/01.rli.0000312922.22136.7f> (2008).
14. Edin, C. et al. Ectopic fat is associated with cardiac remodeling—a Comprehensive assessment of regional fat depots in type 2 diabetes using multi-parametric MRI. *Front. Cardiovasc. Med.* <https://doi.org/10.3389/fcvm.2022.859829> (2022).
15. Tran, B. V. et al. Reliability of ultrasound hepatorenal index and magnetic resonance imaging proton density fat fraction techniques in the diagnosis of hepatic steatosis, with magnetic resonance spectroscopy as the reference standard. *Plos One*. **16**, e255768. <https://doi.org/10.1371/journal.pone.0255768> (2021).
16. Rietzler, A. et al. Energy metabolism measured by 31P magnetic resonance spectroscopy in the healthy human brain. *J. Neuroradiol.* **49**, 370–379. <https://doi.org/10.1016/j.neurad.2022.03.002> (2022).
17. Haggag, H. & Hodgson, C. Clinimetrics: Modified rankin scale (Mrs). *J. Physiother.* **68**, 281. <https://doi.org/10.1016/j.jphys.2022.04.001> (2022).
18. Wang, Y., Ju, Y., An, Q., Lin, L. & Liu, A. L. Mdxon-quant for differentiation of renal damage degree in patients with chronic kidney disease. *Front. Endocrinol.* **14**, 1187042. <https://doi.org/10.3389/fendo.2023.1187042> (2023).
19. Li, Q. L. et al. Quantification of testicular fat deposition in the evaluation of middle-aged overweight male infertility. *Magma* **33**, 377–384. <https://doi.org/10.1007/s10019-020-00514-9> (2020).
20. U-Din, M. et al. Characteristics of abdominal visceral adipose tissue, metabolic health and the gut microbiome in adults. *J. Clin. Endocrinol. Metab.* **109**, 680–690. <https://doi.org/10.1210/ncem.2023.30455> (2024).
21. Li, X. et al. Behind BMI: The potential indicative role of abdominal ectopic fat on glucose metabolism. *Obes. Facts*. **17**, 158–168. <https://doi.org/10.1159/000548567> (2024).
22. Chen, Y. et al. Comprehensive assessment of distinct abdominal fat compartments beyond liver content in overweight/obese patients using MRI and ultrasound imaging. *Abdom. Radiol.* <https://doi.org/10.1007/s00664-024-06897-5> (2024).
23. Moran, G. M., Bakhal, C., Song, S. H. & Agwu, J. C. Type 2 diabetes: Summary of updated nice guidance. *BMJ-Br. Med. J.* **377**, o775. <https://doi.org/10.1136/bmj.o775> (2022).
24. Zhang, Y. et al. Comparison of CT and magnetic resonance mdixon-quant sequence in the diagnosis of mild hepatic steatosis. *Br. J. Radiol.* **91**, 20170587. <https://doi.org/10.1259/bjr.20170587> (2018).
25. Patel, N. S. et al. Association between novel MRI-estimated pancreatic fat and liver histology-determined steatosis and fibrosis in non-alcoholic fatty liver disease. *Aliment. Pharmacol. Ther.* **37**, 630–639. <https://doi.org/10.1111/apt.12553> (2013).
26. Levett, E. et al. Ectopic and visceral fat deposition in lean and obese patients with type 2 diabetes. *J. Am. Coll. Cardiol.* **68**, 53–63. <https://doi.org/10.1016/j.jacc.2016.04.041> (2016).
27. Singh, R. G. et al. Intrapancratic fat deposition and visceral fat volume are associated with the presence of diabetes after acute pancreatitis. *Am. J. Physiol.-Gastroint Liver Physiol.* **316**, G806–G815. <https://doi.org/10.1152/ajpgi.00057.2018> (2019).
28. Pan, Z. et al. Enhanced accuracy and stability in automated intra-pancreatic fat deposition monitoring of type 2 diabetes mellitus using dixon MRI and deep learning. *Abdom. Radiol.* <https://doi.org/10.1007/s00664-024-06898-4> (2025).
29. Garg, U. K. et al. Abdominal fat depots and their association with insulin resistance in patients with type 2 diabetes. *Plos One*. **18**, e295492. <https://doi.org/10.1371/journal.pone.0295492> (2023).
30. Dong, Z. et al. Noninvasive fat quantification of the liver and pancreas may provide potential biomarkers of impaired glucose tolerance and type 2 diabetes. *Medicine (Baltimore)*. **95**, 13858. <https://doi.org/10.1097/med.2016.95.27.e3858> (2016).
31. Capitan, V. et al. Macroscopic heterogeneity of liver fat: An Mr-based study in type-2 diabetic patients. *Eur. Radiol.* **22**, 2161–2168. <https://doi.org/10.1007/s00339-011-2266-8> (2012).
32. Chai, J. et al. MRI chemical shift imaging of the fat content of the pancreas and liver of patients with type 2 diabetes mellitus. *Exp. Ther. Med.* **11**, 476–480. <https://doi.org/10.3892/etm-0-0-2697> (2016).
33. Zeng, Q. et al. CT-derived abdominal adiposity: Distributions and better predictive ability than BMI in a nationwide study of 59,429 adults in China. *Metab.-Clin. Exp.* **115**, 154456. <https://doi.org/10.1016/j.metabolism.2021.154456> (2021).
34. Gotoh, K. et al. Spleen-derived interleukin-10 downregulates the severity of high-fat diet-induced non-alcoholic fatty pancreas disease. *Plos One* **7**, e53154. <https://doi.org/10.1371/journal.pone.0053154> (2012).
35. Wang, M. et al. Sleeve gastrectomy ameliorates diabetes-related spleen damage by improving oxidative stress status in diabetic obese rats. *Obes. Surg.* **31**, 1183–1195. <https://doi.org/10.1007/s11695-021-05506-5> (2021).
36. Kaur, J., Khosla, S. & Farr, J. N. Effects of diabetes on osteocytes. *Curr. Opin. Endocrinol. Diabetes Obes.* **29**, 310–317. <https://doi.org/10.1097/00063041-202206000-00004> (2022).
37. Jones, B. C. et al. MRI quantification of cortical bone porosity, mineralization, and morphologic structure in postmenopausal osteoporosis. *Radiology* **307**, e221810. <https://doi.org/10.1148/ry.2022.220002> (2023).
38. Kiefer, L. S. et al. Assessment of the degree of abdominal myosteatosis by magnetic resonance imaging in subjects with diabetes, prediabetes and healthy controls from the general population. *Eur. J. Radiol.* **105**, 261–268. <https://doi.org/10.1016/j.ejr.2018.05.025> (2018).
39. Yu, F. et al. Intermuscular fat content in young Chinese men with newly diagnosed type 2 diabetes: Based On Mr Mdxon-quant quantitative technique. *Front. Endocrinol.* **12**, 536018. <https://doi.org/10.3389/fendo.2021.536018> (2021).
40. Smith, U. Abdominal obesity: A marker of ectopic fat accumulation. *J. Clin. Invest.* **125**, 1790–1792. <https://doi.org/10.1172/jci.86279> (2015).
41. Wan, H. et al. Associations between abdominal obesity indices and diabetic complications: Chinese visceral adiposity index and neck circumference. *Cardiovasc. Diabetol.* **19**, 118. <https://doi.org/10.1186/s12933-020-01186-5> (2020).
42. Tanaka, T. et al. Impact of abdominal fat distribution, visceral fat, and subcutaneous fat on coronary plaque scores assessed by 320-row computed tomography coronary angiography. *Atherosclerosis* **287**, 155–161. <https://doi.org/10.1016/j.atherosclerosis.2019.06.022> (2019).
43. Chen, P. et al. Abdominal subcutaneous adipose tissue: A favorable adipose depot for diabetes. *Cardiovasc. Diabetol.* <https://doi.org/10.1186/s12933-018-0081-1> (2018).

Author contributions

Yuan and Tao focused on writing the article. Ma and Zhang mainly examined the subjects with MR. All the people reviewed the article.

Funding

This work was supported by grants from Tianjin Key Medical Discipline (Specialty) Construction Project (TJYXZDXK-041A) and Natural Science Foundation of Tianjin, China (21JCYJC01050).

Declarations

Competing interests

The authors declare no competing interests.

Additional information

Correspondence and requests for materials should be addressed to Z.C. or Q.J.

Reprints and permissions information is available at www.nature.com/reprints.

Publisher's note Springer Nature remains neutral with regard to jurisdictional claims in published maps and institutional affiliations.

Open Access This article is licensed under a Creative Commons Attribution-NonCommercial-NoDerivatives 4.0 International License, which permits any non-commercial use, sharing, distribution and reproduction in any medium or format, as long as you give appropriate credit to the original author(s) and the source, provide a link to the Creative Commons licence, and indicate if you modified the licensed material. You do not have permission under this licence to share adapted material derived from this article or parts of it. The images or other third party material in this article are included in the article's Creative Commons licence, unless indicated otherwise in a credit line to the material. If material is not included in the article's Creative Commons licence and your intended use is not permitted by statutory regulation or exceeds the permitted use, you will need to obtain permission directly from the copyright holder. To view a copy of this licence, visit <http://creativecommons.org/licenses/by-nc-nd/4.0/>.

© The Author(s) 2025